Blueshifted Raman scattering and its correlation with the [110] growth direction in gallium oxide nanowires

R. Rao and A. M. Rao[a]
Department of Physics and Astronomy, Clemson University, Clemson, South Carolina 29634

B. Xu and J. Dong
Department of Physics, Auburn University, Auburn, Alabama 36849

S. Sharma
1501 Page Mill Road, Hewlett-Packard Laboratories, Palo Alto, California 94304

M. K. Sunkara
Department of Chemical Engineering, University of Louisville, Louisville, Kentucky 40292.

The Raman spectrum of gallium oxide (β-Ga$_2$O$_3$) nanowires with [001] growth direction is identical to that of the bulk Ga$_2$O$_3$ [Y. C. Choi *et al.* Adv. Mater. **12**, 746 (2000)] while that of β-Ga$_2$O$_3$ nanowires with [40$\bar{1}$] growth direction is redshifted by 4–23 cm^{-1} [Y. H. Gao *et al.* Appl. Phys. Lett. **81**, 2267 (2002)]. Here we report the Raman and Fourier transform infrared spectra of β-Ga$_2$O$_3$ nanowires with [110] growth direction which is blueshifted relative to the bulk spectra by $\sim$10–40 cm^{-1}. Based on a first principles calculation of the strain dependence of Raman mode frequencies in bulk β-Ga$_2$O$_3$, we correlate the observed frequency shifts to growth-direction-induced internal strains in the nanowires. © *2005 American Institute of Physics.*
[DOI: 10.1063/1.2128044]

INTRODUCTION

One-dimensional nanostructured forms of β-phase of gallium oxide (β-Ga$_2$O$_3$) such as nanotubes, nanobelts, and nanowires, have attracted recent interest due to enhanced optical[1,2] properties. Recently, Choi *et al.*[3] synthesized β-Ga$_2$O$_3$ nanowires (diameter range of $\sim$15–45 nm) with a [001] growth direction using an arc-discharge method. Gao *et al.*[4] synthesized [40$\bar{1}$] β-Ga$_2$O$_3$ nanowires with diameters ranging from $\sim$10–100 nm in a vertical radio-frequency furnace. Interestingly, the Raman mode frequencies of the [001] β-Ga$_2$O$_3$ nanowires coincide with the corresponding frequencies in bulk β-Ga$_2$O$_3$.[3] On the other hand, the Raman mode frequencies of the [40$\bar{1}$] β-Ga$_2$O$_3$ nanowires are redshifted relative to corresponding frequencies in bulk β-Ga$_2$O$_3$ by 4–23 cm^{-1}.[4] Using plasma-enhanced chemical-vapor deposition, we have synthesized β-Ga$_2$O$_3$ nanowires whose growth is along the [110] direction.[5] This paper focuses on the micro-Raman and Fourier transform infrared (FTIR) characterization of [110] β-Ga$_2$O$_3$ nanowires, and first principle calculations of the Raman mode frequencies under internal strains. Our calculated Raman frequency shifts suggests that the observed shifts in the nanowires with the [40$\bar{1}$] and [110] growth directions can be explained in term of different internal strains, in contrast to the previously suggested quantum confinement effects and defect-induced effects.

[a]Author to whom correspondence should be addressed; electronic mail: arao@clemson.edu

EXPERIMENT

Synthesis of the β-Ga$_2$O$_3$ nanowires was carried out in a microwave plasma reactor (ASTEX 5010) with H$_2$/CH$_4$/O$_2$ gas mixtures. Quartz substrates were covered with a thin film of molten gallium and were exposed to a microwave plasma containing a range of gas phase species. During the plasma exposure, molten gallium flowed on all the substrates, forming a thin film, which was followed by the growth of nanowires. The substrate temperature was measured by an infrared pyrometer to be approximately 550 °C for 700 W microwave power, 40 Torr total pressure, and 8.0 SCCM (standard cubic centimeter per minute) of O$_2$ in 100 SCCM of hydrogen in the inlet stream. The experiments were performed under the following range of growth conditions: microwave power of 600–1200 W, pressure of 30–60 Torr, growth duration of 1–12 h, 0.6–10 SCCM of O$_2$ SCCM of CH$_4$ in 100 SCCM of hydrogen in the feed gas.

RESULTS AND DISCUSSION

Figure 1(a) shows a scanning electron micrograph (SEM) of Ga$_2$O$_3$ nanowires grown from a large molten gallium droplet. Nanowires were seen to be dispersed uniformly over the substrates. Figure 1(b) shows a high-resolution transmission electron micrograph (TEM) of an individual 13-nm-thick single-crystalline Ga$_2$O$_3$ nanowire (nanowire 1). Electron diffraction from the nanowire confirmed its growth direction to be along [110] crystallographic direction. A second nanowire (nanowire 2) is also visible in the vicinity of nanowire 1 on the TEM grid, lying in a different plane tilted with respect to that of nanowire 1. Also, analysis of the x-ray-diffraction patterns (not shown here) yielded a_0
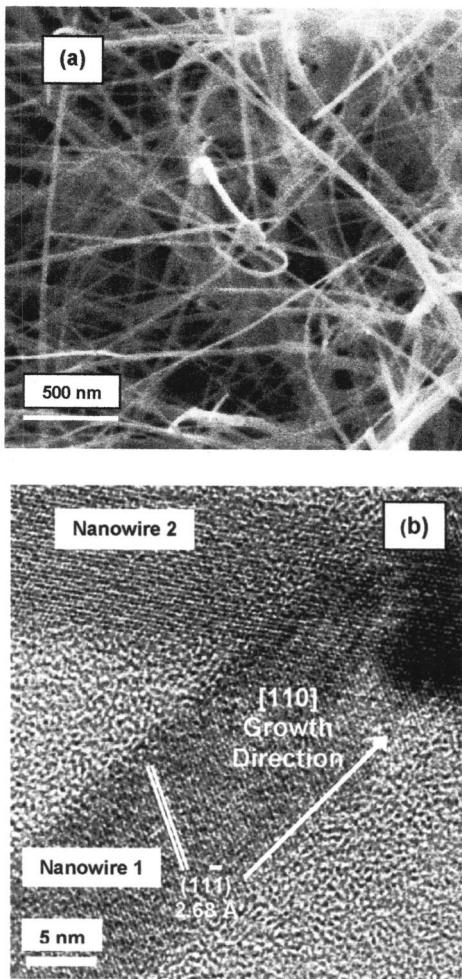
FIG. 1. (a) SEM micrograph of β-Ga$_2$O$_3$ nanowires grown from a large molten gallium droplet using a microwave plasma mediated technique. (b) A high-resolution TEM image of an individual 13-nm-thick β-Ga$_2$O$_3$ nanowire.

FIG. 2. (Color online) Micro-Raman spectra of bulk β-Ga$_2$O$_3$ (bottom trace) and [110] nanowires (top trace).

calculation. A noteworthy point is that no experimental analysis on the mode symmetry of β-Ga$_2$O$_3$ Raman peaks has been reported. Our current mode symmetry assignment is purely based on the comparison between the observed and calculated Raman frequencies. We find an unambiguous matching pattern for mode symmetry assignment for all the observed Raman modes, except for the two Raman peaks around 472 and 629 cm^{-1}. The former peak can be assigned with either the calculated A_g mode of 469 cm^{-1} or the B_g mode of 474 cm^{-1}, while the latter one can be assigned with either the A_g mode of 601 cm^{-1} or the B_g mode of 624 cm^{-1}.[9]

The Raman spectrum of the [110] nanowires, on the other hand is relatively richer compared to the bulk and is significantly *blueshifted* in frequency (Fig. 2). The matching between the Raman peaks in the [110] nanowires and those

$=12.23$ Å, $b_0=3.04$ Å, $c_0=5.8$ Å, $\beta=103.7°$, confirming the presence of a monoclinic β-Ga$_2$O$_3$ phase in these nanowires.

Room-temperature micro-Raman spectrum (785 nm excitation, laser power $\sim$5–10 mW) obtained from [110] β-Ga$_2$O$_3$ nanowires dispersed on quartz is compared with the corresponding spectrum for the bulk material in Fig. 2. β-Ga$_2$O$_3$ has a monoclinic structure and belongs to the C_{2h} space group.[6] Its unit cell contains two formula units-GaO$_6$ (edge sharing) octahedra and GaO$_4$ (corner sharing) tetrahedra and 15 Raman and 12 infrared (IR) active modes are expected in its vibrational spectrum.

The Raman-active modes of β-Ga$_2$O$_3$ can be classified into three groups: high-frequency stretching and bending of GaO$_4$ tetrahedra ($\sim$770–500 cm^{-1}), midfrequency deformation of Ga$_2$O$_6$ octahedra ($\sim$480–310 cm^{-1}), and low-frequency libration and translation (below 200 cm^{-1}) of tetrahedra-octahedra chains.[7] Calculated (described below) and measured Raman mode frequencies for bulk β-Ga$_2$O$_3$ are listed in Table I.[8] Ten Raman peaks are observed in our present study of bulk β-Ga$_2$O$_3$. Our experimental Raman mode frequencies correspond well to those reported in the literature, as well as our local-density approximation (LDA)

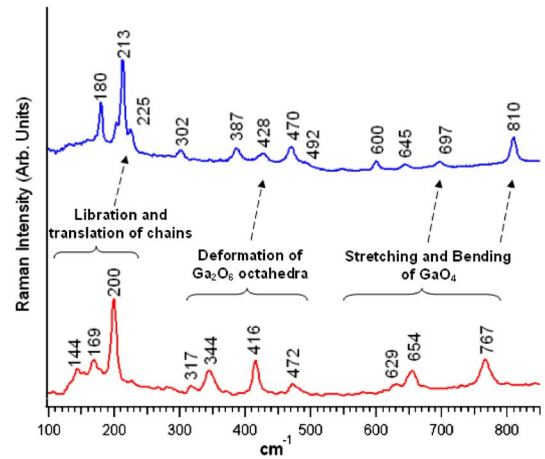TABLE I. Comparison of calculated Raman mode frequencies with those measured in bulk β-Ga$_2$O$_3$.

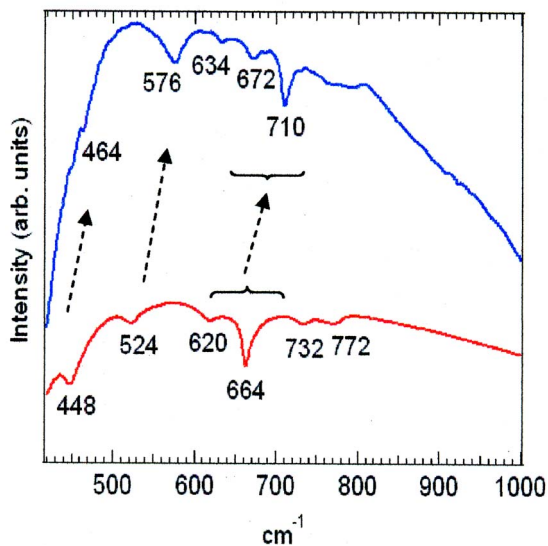| Mode symmetry | Dohy *et al.*[a] | | This work | |
	Empirical calculation (cm^{-1})	Expt. data (cm^{-1})	LDA calculated frequency: (cm^{-1})	Expt. data (cm^{-1})
A_g	113	111	104	…
B_g	114	114	113	…
B_g	152	147	150	144
A_g	166	169	166	169
A_g	195	199	207	200
A_g	308	318	317	317
A_g	353	346	348	344
B_g	360	353	356	…
A_g	406	415	414	416
A_g	468	475	469	472
B_g	474		474	…
A_g	628	628	601	629
B_g	644	651	624	…
A_g	654	657	635	654
A_g	760	763	732	767

[a]Reference 7.

FIG. 3. (Color online) FTIR transmittance spectra of bulk (bottom trace) and [110] β-Ga$_2$O$_3$ nanowires (top trace).

in the bulk is simple for the modes located at either end of the Raman spectra. For the low-frequency libration/translation modes, we can identify the strongest Raman peak at 200 cm^{-1} in the bulk being shifted to 213 cm^{-1} in the nanowires. Accordingly, we attribute the nearby 180 cm^{-1} mode as shifted from the 169 cm^{-1} mode in the bulk. The relatively weaker 144 cm^{-1} bulk Raman peak is invisible in the spectra of the nanowires, likely due to reduction of peak intensity. Meanwhile, a minor peak appears in the low-frequency region of the nanowires spectra at 302 cm^{-1}, which cannot be related to any calculated bulk Raman active modes. Overall, the librational/translational modes are blue-shifted by ~10 cm^{-1}. On the other end of the Raman spectra, two highest-frequency stretching/bending modes of tetrahedra are found to be blueshifted by nearly ~40 cm^{-1}, i.e., 767 cm$^{-1} \rightarrow 810$ cm^{-1} and 654 cm$^{-1} \rightarrow 697$ cm^{-1}. The third highest-frequency Raman peak observed in the nanowires at 645 cm^{-1} is assigned as the blueshifted 629 cm^{-1} mode in the bulk. There is a fourth peak in the high-frequency region (around 600 cm^{-1}). The only possible match for this peak is with the unobserved bulk Raman mode (either the A_g mode of 601 cm^{-1} or the B_g mode of 624 cm^{-1}) predicted by our LDA calculation. While the overall shifting pattern of the Raman peaks in the intermediate frequency ranges is clearly blueshifted, the exact peak-to-peak matching is less clear, partially because several additional weak peaks are also observed which do not correspond to infrared peaks expected in β-Ga$_2$O$_3$.[7] We further confirmed that these additional peaks cannot be attributed to the presence of α-Ga$_2$O$_3$.[10] Tentatively, we assume that the bulk modes at 416 and 472 cm^{-1} are shifted to 428 and 492 cm^{-1}, respectively. As discussed in the following section of theoretical results, this assumption is consistent with our LDA calculations. However, we do not provide explanations for the appearance of additional peaks in this frequency region.

Figure 3 shows the corresponding FTIR transmittance spectra for the same samples whose micro-Raman spectra appear in Fig. 2. FTIR transmittance spectra were obtained using a Bruker IFS 66 v/s spectrometer from pressed KBr pellets containing dispersions of either powder or nanowire forms of β-Ga$_2$O$_3$. Consistent with the Raman spectrum (Fig. 2), the IR modes in the nanowire spectrum are also blueshifted in frequency relative to corresponding bulk frequencies. The IR mode frequencies above 600 cm^{-1} in β-Ga$_2$O$_3$ nanowires are blueshifted in frequency by as much as 50 cm^{-1}.

The blueshift in phonon frequencies of low-dimensional materials are often attributed to the size-confinement effect.[11,12] However, the average diameter of our β-Ga$_2$O$_3$ nanowires is around 25 nm. It is unlikely that the quantum size confinement at this length scale is significant enough to cause the phonon shifts as large as 50 cm^{-1}. Furthermore, three distinctly different shift patterns have been experimentally observed for the β-Ga$_2$O$_3$ nanowires of different growth directions. In contrast to the blueshift in the Raman and FTIR spectra reported in this paper, Choi *et al.* showed that their Fourier transform Raman spectrum of [001] β-Ga$_2$O$_3$ nanowires to be identical to that of bulk β-Ga$_2$O$_3$,[3] while Gao *et al.* exhibited a *redshift* of 4–23 cm^{-1} in the Raman peak frequencies of their [40$\bar{1}$] β-Ga$_2$O$_3$ nanowires relative to the corresponding Raman frequencies in bulk β-Ga$_2$O$_3$.[2] The size confinement effect is clearly insufficient to explain the diversity of the observed shift patterns.

On the other hand, the redshift in the phonon frequencies has also been attributed to the presence of impurities and defects, such as point defects, twins, and stacking faults.[13] These defects are also likely to be responsible for additional vibrational modes observed in the Raman spectra (and to a small extent in the FTIR spectrum) of nanowires. From a detailed high-resolution transmission electron micsoscopy (HRTEM) study, Gao *et al.* confirmed the presence of twins and edge dislocations in their nanowires.[4] Dai *et al.*[14] also proposed that the O vacancies and the stacking faults caused an abnormality in the Ga–O bond vibration and led to redshift in the Raman frequencies. Although this simple hypothesis is plausible, there is one obvious weakness, i.e., lack of close correlation between defect types and the growth directions. Presumably, similar defects might exist in the nanowires with different growth directions. It is also not clear which types of defects will lead to a blueshift in vibrational frequencies. Moreover, different regions in the nanowires contain different defects which would imply that different shifts in the Raman and/or IR spectra should be observed when different regions of the *same* nanowire are probed. However, this does not seem to be the case and instead overall distinct blueshifts or redshifts have been observed for a given nanowire. Therefore, alternative models that are capable of describing these diverse peak-shift patterns in a consistent fashion are needed.

Based on a first principles calculation which we describe next, we propose that the phonon frequencies in different β-Ga$_2$O$_3$ nanowires are shifted as a result of internal strains in the nanowire. The basic assumption of our model is the presence of non-negligible internal strains in the nanowires due to their large surface/volume ratio. Different growth directions will cause different surface reconstruction, and con-

TABLE II. Estimated internal strains.

Strain	[110] nanowire	[40$\bar{1}$] nanowire
ε_{11}	−0.0077	0.0029
ε_{22}	0.0180	−0.0064
ε_{33}	−0.0311	0.0106
ε_{13}	0.0233	−0.0256
$\Delta V/V$	−0.0208	0.0071

sequently lead to internal strains of different magnitudes and directions. This model provides a consistent explanation for all three aforementioned Raman spectra.

Direct first principles calculations of phonon frequencies of 25-nm-diam nanowires is a computationally challenging task as large supercell models (of at least tens of thousands of atoms) are needed. Instead, our current computation study focuses on providing a quantitative estimation of the internal strains which can account for the observed blue- and red-shifts in the Raman frequencies for [110] and [40$\bar{1}$] β-Ga$_2$O$_3$ nanowires, respectively. We have calculated the strain dependences of the *bulk* β-Ga$_2$O$_3$ using a density-functional theory (DFT) method.[15] The internal strains of the nanowires were estimated based on the least-squares fitting of the experimentally observed Raman frequency shifts with theoretically predicted linear strain coefficients $d\omega/d\varepsilon_{ij}$, where ω and ε_{ij} are Raman frequencies and components of strain tensors, respectively.

The Γ-point phonons of bulk β-Ga$_2$O$_3$ were calculated with a real-space finite-displacement technique.[16] Such calculations have been used extensively for describing the structural and vibrational properties of ceramic oxides, nitrides, and carbides.[17] Because of its C_{2h} space-group symmetry, the LO-TO splittings in the optic modes of β-Ga$_2$O$_3$ only exist for the infrared (A_u and B_u) phonon modes, not the Raman active (A_g and B_g) phonon modes. Therefore, all our Raman frequency calculations of β-Ga$_2$O$_3$ were carried out with 10-atom base-centered monoclinic unit-cell model without the correction for the macroscopic interaction. As shown in Table I, the theoretical data for bulk β-Ga$_2$O$_3$ matches well with 13 out of the 15 Raman active ($10A_g+5B_g$) modes observed in present study, as well as those of the previous study of Dohy *et al.*[7] In both cases of the unobserved Raman modes, there is another Raman active mode in the close proximity. For example, our LDA calculations predicted two Raman modes at 469 and 474 cm^{-1}, and two Raman modes at 601 and 629 cm^{-1}. This suggests that it is possible that the two "missing" Raman modes are hidden by the stronger adjacent Raman modes.

The strain tensor of this monoclinic crystal has six independent elements, $\varepsilon_{11}, \varepsilon_{22}, \varepsilon_{33}, \varepsilon_{23}, \varepsilon_{13}$, and ε_{12}. For simplicity, we restricted this study to linear effects, i.e., $\omega(\varepsilon) \approx \omega_0 + \Sigma(d\omega/d\varepsilon_{ij} \times \varepsilon_{ij})$. This approximation is valid for small strains. We further neglected the strain of ε_{23} or ε_{12} because their $d\omega/d\varepsilon_{ij}$ coefficients are zeroes due to the monoclinic lattice symmetry. For each of four remaining types of strains ($\varepsilon_{11}, \varepsilon_{22}, \varepsilon_{33}$, and ε_{13}), the Raman frequencies were calculated for five finite strain values between −0.02 and +0.02. The calculated frequencies were then fitted with a polynomial function to obtain the linear strain coefficients.

Fitting the experimental data within our strain-induced phonon shifts model, we predict the internal strains in nano-

TABLE III. Raman mode frequencies and frequency shifts in β-Ga$_2$O$_3$ nanowires with the [40$\bar{1}$] and [110] growth directions. Overall, excellent agreement between the observed and calculated shifts is seen for all mode frequencies except the one marked with an *.

Gao *et al.*[a] [40$\bar{1}$] growth direction				This work [110] growth direction			
Bulk frequencies (cm^{-1})	Nanowire frequencies (cm^{-1})	Frequency shifts $\Delta\omega$ (cm^{-1})	Calculated frequency shifts (cm^{-1})	Bulk frequencies (cm^{-1})	Nanowire frequencies (cm^{-1})	Frequency shifts $\Delta\omega$ (cm^{-1})	Calculated frequency shifts (cm^{-1})
			−4.8				12.0
			1.7				−3.1
142	134	−8*	−1.0	144			3.8
167	160	−7	−7.2	169	180	+11	10.6
198	194	−4	−6.5	200	213	+13	13.5
320			−3.9	317			9.5
344	332	−12	−6.7	344			16.8
			−1.7				0.7
415	409	−6	−5.3	416	428	+12	12.3
473			−4.4	472	492	+20	21.1
			−6.2				18.5
627			−5.7	629	645	+16	17.8
			−0.3				3.6
651	641	−10	−14.8	654	697	+43	36.4
765	742	−23	−20.6	767	810	+43	47.0

[a]Reference 4.

wires which showed the three distinct Raman spectra. The results of the $[40\bar{1}]$ and $[110]$ nanowires are listed in Table II, and our model predicts the strain tensor for the $[001]$ nanowires contain non-negligible $\varepsilon_{11}, \varepsilon_{22}, \varepsilon_{33}$, and ε_{13} components. As shown in Table III, we obtain overall excellent fits for both the redshifted and blueshifted Raman spectra, with exception of the 134 cm^{-1} B_g mode in the $[40\bar{1}]$ nanowire (Gao *et al.*). Our calculation shows that the $[110]$ nanowire is compressed along its a and c axis, and stretched along its b axis. The strain in the $[40\bar{1}]$ nanowire exhibits a contrasting pattern and its strain magnitude is only about 1/3 of that evaluated for the $[110]$ nanowire. In both cases, the a axis has the smallest change (Table II). The strain-induced volume changes are predicted to be −2% and 0.7% for the $[110]$ and $[40\bar{1}]$ nanowires, respectively. Seo *et al.*[18] studied the internal strains of GaN nanowires using x-ray measurements and they reported the strains of $\varepsilon_{xx}=2.3\%$, $\varepsilon_{yy}=-0.734\%$, and $\varepsilon_{zz}=-0.4\%$ based on their experimental x-ray measurement. The magnitudes of our predicted strains of β-Ga$_2$O$_3$ are comparable to those of GaN nanowires.

CONCLUSIONS

In summary, based on a comparison of the experimental Raman mode frequencies with our first-principles calculations, we find compelling evidence for growth direction-induced internal strains in β-Ga$_2$O$_3$ nanowires which significantly influence the vibrational mode frequencies. Within the linear model approximation, the observed blue and redshifts of peak frequencies in the micro-Raman spectra of the β-Ga$_2$O$_3$ nanowires with different growth directions can be attributed to two small anisotropic internal strains: one compressive strain of 2% volume change, and the other tensile strain of 0.7% volume change. The overall high quality of the fitted models to available experimental data suggests a strong correlation between the shifts in Raman mode frequencies and the growth direction-induced internal strains in the Ga$_2$O$_3$ nanowires.

[1]G. Gundiah, A. Govindaraj, and C. N. R. Rao, Chem. Phys. Lett. **351**, 189 (2002).

[2]C. H. Liang, G. W. Meng, G. Z. Wang, Y. W. Wang, and L. D. Zhang, Appl. Phys. Lett. **78**, 3202 (2001).

[3]Y. C. Choi *et al.*, Adv. Mater. (Weinheim, Ger.) **12**, 746 (2000).

[4]Y. H. Gao, Y. Bando, and T. Sato, Appl. Phys. Lett. **81**, 2267 (2002).

[5]S. Sharma and M. K. Sunkara, J. Am. Chem. Soc. **124**, 12288 (2002).

[6]S. Geller, J. Chem. Phys. **33**, 676 (1960).

[7]D. Dohy, G. Lucazeau, and A. Revcolecschi, J. Solid State Chem. **45**, 180 (1982).

[8]Bulk Raman spectrum was obtained from β-Ga$_2$O$_3$ polyhedra that were cosynthesized in unoptimized runs.

[9]Our results assigned the lower frequency 469 cm^{-1} mode as an A_g mode and the higher frequency 474 cm^{-1} mode as the B_g mode. This assignment is contradictory to the previous report of Dohy *et al.*, who assigned the 468 cm^{-1} mode as the B_g mode and the 474 cm^{-1} mode as the A_g mode based on an empirical calculation.

[10]K. Fukumi and S. Sakka, Phys. Chem. Glasses **29**, 1 (1988).

[11]J. Rubio *et al.* H. P. Van der Meuler, Solid-State Electron. **40**, 707 (1996).

[12]A. K. Arora, T. R. Ravindran, G. L. N. Reddy, A. K. Sikder, and D. S. Misra, Diamond Relat. Mater. **10**, 1477 (2002).

[13]S-L. Zhang, B-F. Zhu, F. Huang, Y. Yan, E. Shang, S. Fan, and W. Han, Solid State Commun. **111**, 647 (1999).

[14]L. Dai, X. L. Chen, X. N. Zhang, A. Z. Lin, T. Zhou, B. Q. Hu, and Z. Zhang, J. Appl. Phys. **92**, 1062 (2002).

[15]The implementation of DFT adopted in this study is VASP (Vienna Ab-Initio Simulation Package). We chose the LDA for the many-electron exchange-correlation interaction. The valence electrons (i.e., $3d^{10}4s^24p^1$ electrons in Ga and $2s^22p^4$ electrons in O) are treated explicitly in the electron eigenfunction calculations, while the core electrons are approximated with the Vanderbilt-type ultrasoft pseudopotentials. Using a plane-wave energy cutoff of 397.5 eV and a Brillouin zone summation of a 6 $\times 6 \times 6$ Monkhorst-Pack k-point grid, our calculations predict equilibrium lattice parameters for bulk β-Ga$_2$O$_3$ as $a_0=12.11$ Å, $b_0=3.005$ Å, $c_0=5.731$ Å, and $\beta=103.72°$.

[16]J. Dong and A. B. Chen, in *SiC Power materials: Devices and Applications*, edited by F. C. Feng, (Springer-Verlag, Berlin 2004), pp. 63–87, and references therein.

[17]J. Dong and O. F. Sankey, J. Appl. Phys. **87**, 958 (2000); S. Deb, J. Dong, H. Hubert, P. F. McMillan, and O. F. Sankey, Solid State Commun. **114**, 137 (2000).

[18]H. K. Seo, S. Y. Bae, J. Park, H. Yang, K. S. Park, and S. Kim, J. Chem. Phys. **116**, 9492 (2002).